

Prevalence of *CYLD* mutations in Vietnamese patients with polycythemia vera

Do Thi Trang^{1,A–C}, Nguyen Hoang Giang^{1,A–C}, Bui Kieu Trang^{1,B,C}, Nguyen Thy Ngoc^{2,B,C,F},
 Nguyen Van Giang^{4,C,E}, Nguyen Xuan Canh^{4,C,E}, Nguyen Ba Vuong^{5,E,F}, Nguyen Thi Xuan^{1,3,A,C–F}

¹ Institute of Genome Research, Vietnam Academy of Science and Technology, Hanoi, Vietnam

² Department of Life Sciences, University of Science and Technology of Hanoi, Vietnam Academy of Science and Technology, Vietnam

³ Faculty of Biotechnology, Graduate University of Science and Technology, Vietnam Academy of Science and Technology, Hanoi, Vietnam

⁴ Faculty of Biotechnology, Vietnam National University of Agriculture, Hanoi, Vietnam

⁵ 103 Hospital, Vietnam Military Medical University, Hanoi, Vietnam

A – research concept and design; B – collection and/or assembly of data; C – data analysis and interpretation;

D – writing the article; E – critical revision of the article; F – final approval of the article

Advances in Clinical and Experimental Medicine, ISSN 1899–5276 (print), ISSN 2451–2680 (online)

Adv Clin Exp Med. 2022;31(4):369–380

Address for correspondence

Nguyen Thi Xuan
 E-mail: xuannt@igr.ac.vn

Funding sources

This research was funded by the 562 program of the Ministry of Science and Technology for the field of Life Science under grant No. ĐTDLCN.43/21.

Conflict of interest

None declared

Received on August 26, 2021

Reviewed on September 24, 2021

Accepted on November 17, 2021

Published online on January 13, 2022

Cite as

Trang DT, Giang NH, Trang BK, et al. Prevalence of *CYLD* mutations in Vietnamese patients with polycythemia vera. *Adv Clin Exp Med*. 2022;31(4):369–380. doi:10.17219/acem/144027

DOI

10.17219/acem/144027

Copyright

Copyright by Author(s)

This is an article distributed under the terms of the Creative Commons Attribution 3.0 Unported (CC BY 3.0) (<https://creativecommons.org/licenses/by/3.0/>)

Abstract

Background. Polycythemia vera (PV) is characterized by increased proliferation and accumulation of erythroid and mature myeloid cells and megakaryocyte in the bone marrow and peripheral blood. The JAK2V617F mutation is present in most PV patients. Deubiquitinase (DUB) genes, including *TNFAIP3* (*A20*), *CYLD* and *Cezanne*, function as negative regulators of inflammatory reaction through nuclear factor kappa-light-chain-enhancer of activated B cells (NF-κB) signaling.

Objectives. To determine single nucleotide polymorphisms (SNPs) profiling and gene expression of the DUB genes as well as the immunophenotype of PV cells.

Material and methods. Seventy-seven patients with PV and 55 healthy individuals with well-characterized clinical profiles were enrolled. Gene expression profile was determined using quantitative real-time polymerase chain reaction (qRT-PCR), the immunophenotype with flow cytometry, secretion of cytokines using enzyme-linked immunosorbent assay (ELISA), and gene polymorphisms using direct DNA sequencing.

Results. Inactivation of *A20*, *CYLD* and *Cezanne*, and increases in interleukin 6 (IL-6) and tumor necrosis factor alpha (TNF-α) levels, as well as the enhanced number of CD25⁺CD4⁺ T, Th1 and regulatory T cells were observed in PV patients. The genetic analysis of the *CYLD* gene identified 11 SNPs, in which a novel W736G nsSNP in exon 15 and a SNP c.2483+6 T>G in intron 15 were observed in PV cases with the frequencies of 18.2% and 5.2%, respectively. The W736G non-synonymous SNP (nsSNP) was found to be most likely to exert deleterious effect and the intronic SNP c.2483+6 T>G was identified as aberrant splicing. Sequencing of *Cezanne* gene identified 7 SNPs in intron 10 and PV carriers of the SNPs had at least 2 SNPs in this gene. Importantly, PV carriers of the W736G nsSNP had multiple SNPs in *CYLD*, but not in *A20* or *Cezanne* gene.

Conclusions. Two identified SNPs, including the W736G nsSNP and the SNP c.2483+6 T>G, in *CYLD* gene might be associated with a risk of PV disease, in which the deleterious effect of the W736G nsSNP in *CYLD* gene could contribute to the pathogenesis of PV.

Key words: *JAK2*, *CYLD*, *A20*, *Cezanne*, polycythemia vera

Background

Polycythemia vera (PV) is one of the classic Philadelphia chromosome/BCR-ABL1 negative myeloproliferative neoplasms (MPNs) characterized by increased proliferation and accumulation of erythroid and mature myeloid cells and megakaryocyte in the bone marrow and peripheral blood, with subsequent increases in hematocrit and hemoglobin, and overproduction of red blood cells.^{1,2} The most serious complication of PV are the symptoms of thrombosis and cardiovascular disease (CVD), which are major causes of the morbidity and mortality in these patients. The V617F activating mutation in exon 12 of the tyrosine kinase *JAK2* gene frequently occurs in PV patients³ and constitutively induces persistent activation of Janus kinase and signal transducer and activator of transcription (JAK-STAT) pathway in hematopoietic cell precursors to promote multiple cellular processes, including survival, differentiation and proliferation.⁴ In addition to the common *JAK2*V617F mutation, the *MPL*W515L/K and calreticulin (*CALR*) exon 9 indel mutations within the JAK/STAT signaling pathway were also shown to increase the risk of the disease.⁵

Deubiquitinases (DUB) genes, which include tumor necrosis factor alpha (TNF- α)-induced protein 3 (*TNFAIP3*, *A20*), tumor suppressor cylindromatosis (*CYLD*) and *Cezanne*, play important roles in deubiquitinating target proteins by cleaving their polyubiquitin chains to suppress activation of downstream signaling pathways. Lack of *A20* or *CYLD* in mouse immune cells results in constitutive activity of several pathways, including nuclear factor kappa-light-chain-enhancer of activated B cells (NF- κ B) and signal transducer and activator of transcriptions (STATs).^{6,7} In humans, inactivation of *A20* leads to the progression of lymphomas by inducing the proliferation of lymphoma cells.^{8,9} Mutations in exon 3 of *A20* gene cause the risk of malignant T-cell acute lymphoblastic leukemia (T-ALL)¹⁰ and chronic lymphocytic leukemia (CLL).¹¹ Genetic aberration and reduced expression of *CYLD* gene are related to solid cancers and lymphoblastic leukemia.^{12–15} The presence of *CYLD* is known to promote cell death in ALL and CLL cells.^{16,17} Patients having a 9 nucleotide deletion in exon 7 and a single nucleotide substitution in exon 10 of *CYLD* gene are at risk of B-cell acute lymphoblastic leukemia (B-ALL).¹² The *CYLD* expression is inhibited by miR-19 in T-ALL, while miR-19 is highly expressed in leukemia and several tumor cell lines.¹⁸ Similar to *A20* and *CYLD*, *Cezanne* inhibits NF- κ B signaling by deconjugating K63-polyubiquitin chain,¹⁹ and *Cezanne* inactivation is associated with the progression and poor prognosis in hepatocellular carcinoma.²⁰ In contrast, *Cezanne* enhances tumor progression in lung squamous carcinoma and adenocarcinoma.²¹

Several investigations on immune features indicated that *A20* and *CYLD* participate in suppressing inflammatory reaction and accumulation of leukocytes in systemic organs,^{6,7} which is associated with risk for the development

of cancers.²² The *A20*-deficient mice develop severe inflammation and cachexia by recruitment of activated lymphocytes, granulocytes and macrophages into liver and spleen.²³ The *CYLD*-knockout mice exhibit abnormalities in the activation and development of T cells and B cells.^{24,25} In PV patients, regulatory T (Treg) cells are expanded to suppress function of immune effector cells, therefore contributing to the pathogenesis of PV.²⁶

Objectives

In this study, single nucleotide polymorphisms (SNPs) profiling and gene expression of *A20*, *CYLD* and *Cezanne* genes in 77 patients with PV and 55 healthy individuals using direct DNA sequencing and quantitative real-time polymerase chain reaction (qRT-PCR) were performed to determine disease-associated SNPs in the DUB genes. Besides, immunophenotypic property of PV cells was also assessed with flow cytometry.

Materials and methods

Patients and control subjects

Total peripheral blood samples from 77 untreated PV patients with a median age of 58.7 (19–81) years and 55 normal healthy volunteers used as controls were taken at the 103 Hospital, Military Medical University, Hanoi, Vietnam. The diagnosis of PV was based on the 2016 WHO criteria.² The presence of *JAK*V617F mutation in PV patients was determined according to Baxter et al.²⁷ No individuals in the control population took any medication or suffered from any known acute or chronic disease. All patients and volunteers gave a written consent to participate in the study. All care and experimental procedures were performed according to the Vietnamese law on the welfare of patients and were approved by the Ethical Committee of Institute of Genome Research, Vietnam Academy of Science and Technology, Hanoi, Vietnam. All experimental protocols on human subjects were in accordance with 1975 Declaration of Helsinki, as revised in 2008.

Isolation of PV cells and PBMCs

The PV cells from PV patients and peripheral blood mononuclear cells (PBMCs) from healthy donors were collected by venipuncture and transferred to sterile tubes containing ethylenediaminetetraacetic acid (EDTA) as an anticoagulant and isolated using density gradient centrifugation (Ficoll-Paque Plus; GE Healthcare Life Sciences, Chicago, USA). The cells were next counted in a Neubauer chamber, washed with phosphate-buffered saline (PBS) and analyzed for further experiments.

Cytokine quantification

Sera were isolated from the blood samples of PV patients and healthy subjects and stored at -20°C until being used for enzyme-linked immunosorbent assay (ELISA). The TNF- α , interleukin 6 (IL-6) and IL-1 β concentrations were determined using ELISA kits (Thermo Fisher Scientific, Waltham, USA) according to the manufacturer's protocol.

RNA extraction and RT-PCR

Total mRNA was isolated using the QIAshredder and RNeasy Mini Kit from Qiagen (Hilden, Germany), according to the manufacturer's instructions. For cDNA first strand synthesis, 1 μg of total RNA in 12.5 μL of diethyl pyrocarbonate (DEPC)- H_2O was mixed with 1 μL of oligo-dT primer (500 $\mu\text{g}/\text{mL}$; Invitrogen, Waltham, USA) and heated for 2 min at 70°C . To determine transcript levels of *A20*, *Cezanne*, *CYLD*, *OTUB-1*, *OTUB-2*, and *GAPDH*, qRT-PCR with the LightCycler System (Roche, Basel, Switzerland) was applied. The following primers were used: *A20* primers: 5'-TCCTCAGGCTTTGTATTTGA-3' (forward) and 5'-TGTGTATCGGTGCATGGTTT-3' (reverse); *OTUB-1* primers: 5'-ACAGAAGATCAAGGACCTCCA-3' (forward) and 5'-CAACTCCTTGCTGTCATCCA-3' (reverse); *OTUB-2* primers: 5'-CTCACGTCCGGCCTTCATCA-3' (forward) and 5'-GCCATGGGCTCTACTTCGT-3' (reverse); *Cezanne* primers: 5'-ACAATGTCCGATGGCCAGT-3' (forward) and 5'-ACAGTGGGATCCACTTCACATTC-3' (reverse); *CYLD* primers: 5'-TGCCTTCCAACCTCTCGTCTTG-3' (forward) and 5'-AATCCGCTCTTCCCAGTAGG-3' (reverse), and *GAPDH* primers: 5'-GGAGCGAGATCCCTCCAAA-3' (forward) and 5'-GGCTGTTGTCATACTTTCAT-3' (reverse). The qRT-PCR reactions were performed in a final volume of 20 μL containing 2 μL of cDNA, 2.4 μL of MgCl_2 (3 μM), 1 μL of primer mix (0.5 μM of both primers), 2 μL of cDNA SYBR Green I Master mix (Roche), and 12.6 μL of DEPC-treated water. The target DNA was amplified during 40 cycles of 95°C for 10 s, 62°C for 10 s and 72°C for 16 s, each with a temperature transition rate of $20^{\circ}\text{C}/\text{s}$, a secondary target temperature of 50°C and a step size of 0.5°C . Melting curve analysis was performed at 95°C (0 s), 60°C (10 s) and 95°C (0 s) to determine the melting temperature of primer dimers and the specific qRT-PCR products. The ratio between the respective gene and corresponding *GAPDH* was calculated per sample according to the $\Delta\Delta$ cycle threshold method.²⁸

DNA sequencing of *JAK2* and the DUB genes

Genomic DNA was isolated from peripheral blood samples using a DNeasy blood and tissue kit (Qiagen). To determine the polymorphisms of the *JAK2*, *A20*, *CYLD*, and *Cezanne* genes, qRT-PCR and DNA sequencing (3500 Genetic

Analyzers; Thermo Fisher Scientific) were performed as previously described.²⁹ The GenBank accession numbers NM_004972.4, NM_00137874.1, NM_001270508.2 and NM_020205.4 were used for DNA sequence analysis of *JAK2*, *CYLD*, *A20* and *Cezanne*, respectively, by using primers: *JAK2-F*: 5'-TCCTCAGAACGTTGATGGCAG-3' and *JAK2-R*: 5'-ATTGCTTTCTCTTTTTCACAAGAT-3'; *CYLD-F*: 5'-TAAGGTCTTGTGCCTGAGCA-3'; *CYLD-R*: 5'-TTCTTTGGCAGCAGAAATCC-3'; *A20-F*: 5'-TGAGCTAATGATGTAAATCTTGTG-3' and *A20-R*: 5'-AGGAGGCCTCTGCTGTAGTC-3'; *Cezanne-F*: 5'-GCCTCCTGCATCAACTTCCT-3' and *Cezanne-R*: 5'-TCAGAGGACAGTGGGATCCA-3. The amplification product lengths of *JAK2*, *CYLD*, *A20*, and *Cezanne* were 453 bp, 546 bp, 731 bp, and 600 bp, respectively. All obtained PCR fragments were purified with a GeneJET PCR purification kit (Thermo Fisher Scientific). The PCR products were sequenced on both strands with the same primers as the ones used for the PCR.

Immunostaining and flow cytometry

Immunophenotypic features of PV cells and PBMCs were determined with flow cytometry (FACS Aria Fusion; Becton Dickinson Biosciences, Franklin Lakes, USA), as previously described.³⁰ Cells (2×10^6) were incubated in 100 μL of flow cytometry staining (FACS) buffer (PBS plus 0.1% function control sequence (FCS)) containing fluorochrome-coupled antibodies to CD45, CD3, CD4, CD8 α , CD11b, CD25, CD44, and FoxP3 (all from eBioscience; Thermo Fisher Scientific) at a concentration of 10 $\mu\text{g}/\text{mL}$. For intracellular cytokine staining of IL-4, IL-17 and interferon gamma (IFN- γ), cells were stimulated with phorbol 12-myristate 13-acetate (50 ng/mL; Sigma-Aldrich, St. Louis, USA) and ionomycin (500 ng/mL; Sigma-Aldrich) for 3 h, followed by addition of brefeldin A (10 $\mu\text{g}/\text{mL}$; Sigma-Aldrich) for another 4 h. The cells were then stained with anti-human IL-4, IL-17 and IFN- γ antibodies (Thermo Fisher Scientific). After incubating with the antibodies for 60 min at 4°C , the cells were washed twice and resuspended in FACS buffer for flow cytometry analysis.

Data analysis

Data related to the human *JAK2*, *A20*, *CYLD*, and *Cezanne* genes were collected from National Center for Biotechnology Information (NCBI; <https://www.ncbi.nlm.nih.gov/>). The information for SNP ID of these genes was retrieved from the NCBI SNP database (<https://www.ncbi.nlm.nih.gov/snp/>). BioEdit 7.2 software (<https://bioedit.software.informer.com/7.2/>) was used for the initial analysis of the sequences.

To analyze the functional consequence of deleterious SNPs of the DUB genes, the PolyPhen2 program (<http://genetics.bwh.harvard.edu/pph2/index.shtml>) was used. The PolyPhen-2 score varies from 0.0 (tolerated) to 1.0

(deleterious), in which the SNPs were designated “probably damaging”, “potentially damaging”, “benign”, or “unknown”. In addition, the possible impact of intronic SNPs on splicing was predicted using SD-Score (https://www.med.nagoya-u.ac.jp/neurogenetics/SD_Score/sd_score.html)³¹ or MaxEntScan (http://hollywood.mit.edu/burgelab/maxent/Xmaxent_scan_scoreseq.html)³² predictor programs.

Statistical analyses

The IBM SPSS v. 20 software (IBM Corp., Armonk, USA) was used for statistical analysis. The χ^2 test was used to test whether allele distribution of each SNP follows the Hardy–Weinberg equilibrium (HWE). To examine the genotype association of control and PV groups, the Fisher’s exact test was used for SNPs with expected sample sizes less than 20 and χ^2 test for those with larger expected sample sizes. Differences between control and PV groups or SNP relevance were tested for significance using Mann–Whitney U test or Kruskal–Wallis test (for many comparisons). All of the statistical tests were two-sided and represented the number of independent experiments. In all statistical analyses, the significance was determined at the level of $p < 0.05$.

Results

Analysis of gene expression and immunophenotypic profiles in PV patients

For expression of the DUB genes, we observed that mRNA levels of *A20*, *CYLD* and *Cezanne* were significantly downregulated in PV cells as compared to the control group; however, no difference in transcript expression of the other DUB genes, including *OTUB-1* and *OTUB-2*, between patient and control groups was detected (Fig. 1A). The inactivated expression of *A20*, *CYLD* and *Cezanne* is predicted to be caused by their genetic alterations in PV.

Inactivation of the DUBs may lead to constitutive activation and recruitment of immune cells into systemic organs^{6,7}; therefore, changes in the number and activation of myeloid (CD11b⁺) and CD4 T cells present in PV cells were examined. In our results, CD45⁺ cells considered as leukocytes were gated in all experiments. Flow cytometry analysis showed that the percentage of CD11b⁺ myeloid and CD3⁺ T cells were increased in blood circulation of PV patients (Fig. 1B,E). However, the activation of CD11b⁺ myeloid cells in PV cases was found to be similar to that in healthy individuals, as the number of CD11b⁺CD86⁺ and CD11b⁺CD40⁺ expressing cells remained unaltered in these patients (Fig. 1B,C). Unlike CD11b⁺ myeloid cells, the activation of CD3⁺CD4⁺ T cells was partially enhanced, as the number of CD3⁺CD4⁺CD25⁺ (CD25⁺CD4⁺ T cells), but not CD3⁺CD4⁺CD44⁺ (CD44⁺CD4⁺ T cells) was significantly increased in PV cases (Fig. 1D,E).

Next, analysis of CD4 T cells subsets showed that the CD3⁺CD4⁺CD25⁺ FoxP3⁺ (Treg) and CD3⁺CD4⁺IFN- γ ⁺ (Th1) expressing cells were recruited into the circulation, whereas the number of CD3⁺CD4⁺IL-4⁺ (Th2) and CD3⁺CD4⁺IL-17⁺ (Th17) expressing cells was unaltered in PV cases (Fig. 1F,G). In agreement with a previous study, Treg cells are recruited to circulatory system to facilitate the development of PV,²⁶ suggesting that the inactivated expression of *A20*, *CYLD* and *Cezanne* genes in PV patients could be involved in the recruitment of CD25⁺ CD4⁺ T, T regulatory and Th1 cells into blood.

The *A20* and *CYLD* are also known as inhibitors of inflammatory reaction^{7,33}; thus, cytokine production in sera of PV patients was examined. Similar to a recent study,³⁴ we also observed that levels of IL-6 and TNF- α in PV patients were found to be higher than in control individuals; however, these patients showed no change in the serum level of IL-1 β (Fig. 1H).

Mutational analysis of *JAK2* and DUB genes in PV patients

Firstly, the p.V617F (c.1849 G>T) mutation of *JAK2* gene is well known to be pathogenic, has been identified in about 90% PV cases³ and is used as an important diagnostic marker of PV. In this study, the results indicated that 51 out of 77 (66.23%) untreated PV cases were positive with the *JAK2*V617F (Fig. 2A and Table 1,2).

Sequencing of the *CYLD* gene identified 6 nucleotide changes in exon 15 (Fig. 2B), in which 5 out of the 6 SNPs, including p.A705P (c.2355 G>C), p.Q731H (c.2435 G>C), p.E735K (c.2445 G>A), p.W736G (c.2448 T>G), and p.E747K (c.2481 G>A), were non-synonymous SNPs (ns-SNPs), causing changes in the amino acid residues, and the remaining SNP p.E723E (c.2411 G>A) was silent. Five intronic nucleotide changes, including 2 SNPs c.2351-118delA and c.2351-31 T>G in intron 14 and 3 SNPs c.2483+6 T>G, c.2483+39 T>G and c.2483+53 G>A in intron 15, were found (Fig. 2C). The genotype distribution of the observed SNPs, except for the 2 SNPs p.E747K and c.2483+53 G>A in *CYLD* gene, were in agreement with HWE. Importantly, we noted that the minor allele frequency (MAF) of the W736G nsSNP was significantly higher in PV group compared to control group ($p = 0.022$), and the difference in the MAFs for the 10 remaining SNPs between the 2 groups was not observed (Table 1).

For determination of susceptibility to PV by evaluating the deleterious effect of the nsSNPs in *CYLD* gene, the results indicated that among the 5 nsSNPs, only the W736G nsSNP was predicted to be probably damaging by PolyPhen-2 with a score of 0.9456 (score range: 0–1; sensitivity: 0.8; specificity: 0.95) (Fig. 2D). Accordingly, the W736G nsSNP might be one of the most deleterious nsSNPs in *CYLD* gene. Moreover, TG genotype of the W736G nsSNP showed higher frequency in PV patients (18.2%) compared to healthy individuals (1.81%; $p = 0.018$, Table 2),

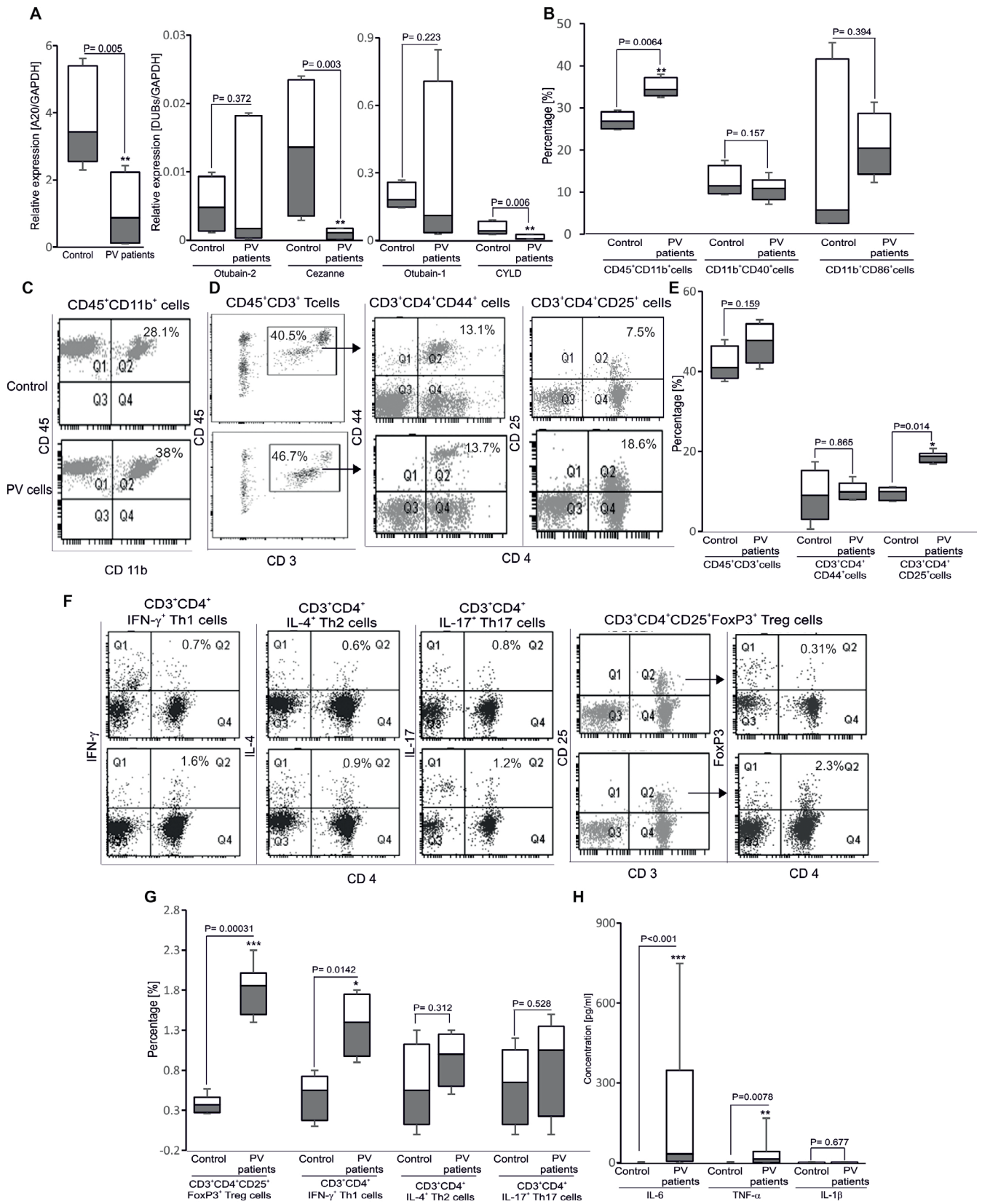


Fig. 1. Gene expression and immunophenotypic feature in polycythemia vera (PV) patients and controls. **A**, Box plot graphs of transcript levels of *A20*, *CYLD*, *OTUB1*, *OTUB2*, and *Cezanne* are shown for control and PV cells; ** ($p < 0.01$) indicates significant difference from healthy individuals (Mann-Whitney U test, $n = 15$). The box plots denote the median, interquartile range (IQR) and minimum and maximum values; **B**, Box plot graphs of percentages of $CD45^+CD11b^+$, $CD11b^+CD40^+$ and $CD11b^+CD86^+$ expressing cells are shown for control and PV cells; ** ($p < 0.01$) indicates significant difference from healthy individuals (Mann-Whitney U test, $n = 5-7$). The box plots denote the median, IQR and minimum and maximum values; **C, D**, Original dot plots of $CD45^+CD11b^+$ (**C**), $CD45^+CD3^+$, $CD3^+CD4^+CD44^+$ and $CD3^+CD4^+CD25^+$ (**D**) expressing cells are shown for control (upper panels) and PV cells (lower panels). All samples were gated with $CD45^+$ live cells; **E**, Box plot graphs of percentages of $CD45^+CD3^+$, $CD3^+CD4^+CD44^+$ and $CD3^+CD4^+CD25^+$ expressing cells are shown for control and PV cells; * ($p < 0.05$) indicates significant difference from healthy individuals (Mann-Whitney U test, $n = 5-7$). The box plots denote the median, IQR and minimum and maximum values; **F**, Original dot plots of $CD3^+CD4^+IFN-\gamma^+$ (Th1), $CD3^+CD4^+IL-4^+$ (Th2) and $CD3^+CD4^+IL-17^+$ (Th17) (gated with $CD45^+CD3^+$) and $CD3^+CD4^+CD25^+FoxP3^+$ (Treg) (gated with $CD45^+CD3^+CD25^+$) expressing cells are shown for control (upper panels) and PV cells (lower panels); **G**, Box plot graphs of percentages of $CD3^+CD4^+IFN-\gamma^+$ (Th1), $CD3^+CD4^+IL-4^+$ (Th2) and $CD3^+CD4^+IL-17^+$ (Th17) and $CD3^+CD4^+CD25^+FoxP3^+$ (Treg) expressing cells are shown for control and PV cells; * ($p < 0.05$) and *** ($p < 0.001$) indicate significant differences from healthy individuals (Mann-Whitney U test, $n = 5-7$). The box plots denote the median, IQR and minimum and maximum values; **H**, Box plot graphs showing interleukin (IL)-6, tumor necrosis factor alpha (TNF- α) and IL-1 β concentrations in sera of healthy donors and PV patients; ** ($p < 0.01$) and *** ($p < 0.001$) indicate significant differences from healthy donors (Mann-Whitney U test, $n = 53-77$). The box plots denote the median, IQR and minimum and maximum values.

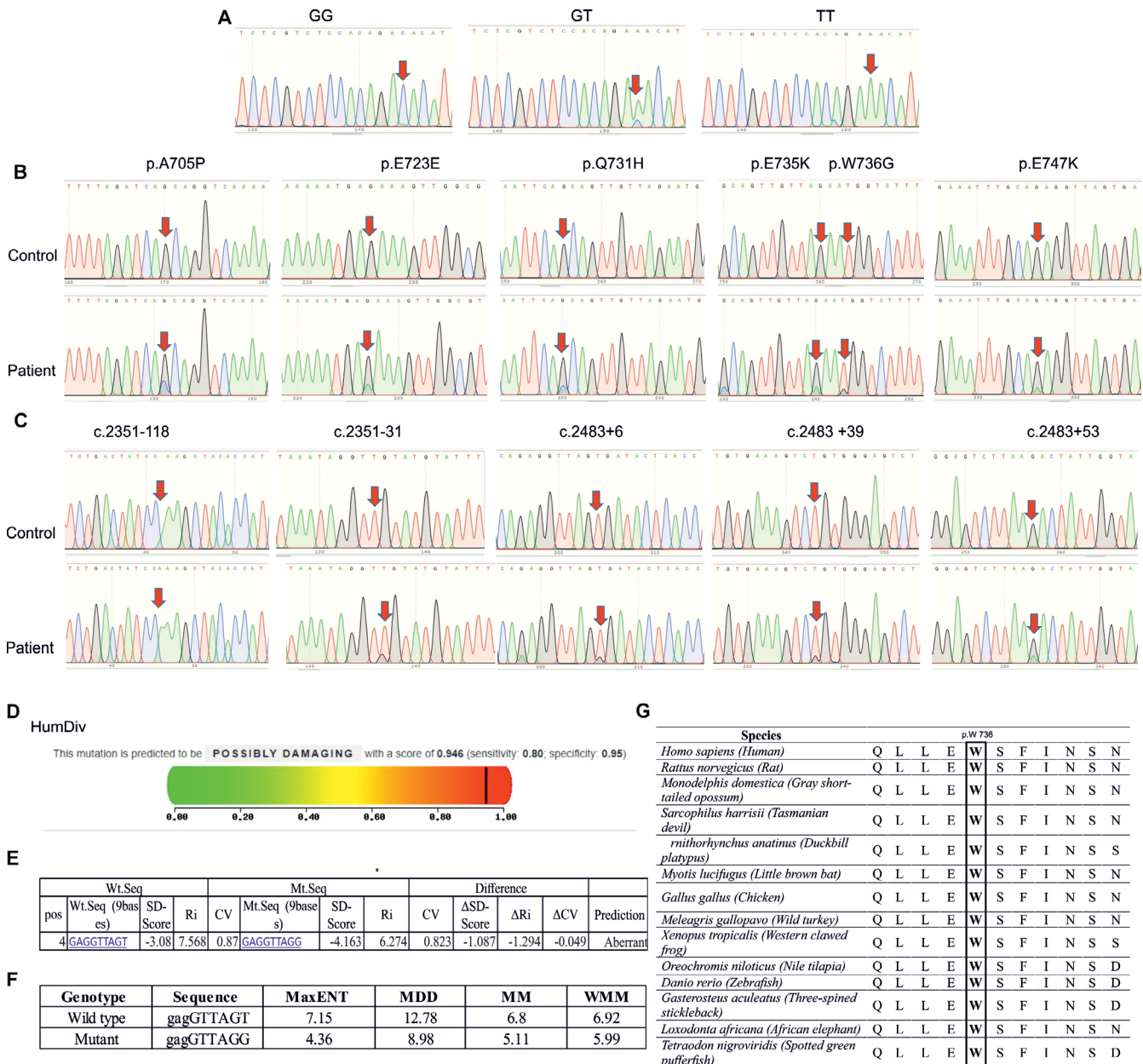


Fig. 2. Polymorphisms of *JAK2* and *CYLD* genes in polycythemia vera (PV) patients and controls. A. Partial sequence chromatograms of *JAK2* gene from healthy individuals (left panel, GG genotype) and PV patients (middle and right panels, GT and TT genotypes) for the p.V617F (c.1849 G>T) mutation. Arrows indicate the location of the base changes; B. Partial sequence chromatograms of *CYLD* gene from healthy individuals (upper panels) and PV patients (lower panels), in which the p.A705P (c.2355 G>C), p.E723E (c.2411 G>A), p.Q731H (c.2435 G>C), p.E735K (c.2445 G>A), p.W736G (c.2448 T>G), and p.E747K (c.2481 G>A) polymorphisms are shown. Arrows indicate the location of the base changes; C. Partial sequence chromatograms of *CYLD* gene from healthy individuals (upper panels) and PV patients (lower panels), in which the c.2351-118delA, c.2351-31 T>G, c.2483+6 T>G, c.2483+39 T>G, and c.2483+53 G>A polymorphisms are shown. Arrows indicate the location of the base changes; D. Functional prediction of the p.W736G mutation using the PolyPhen-2 program; E, F. Splicing effect predictions of the intronic SNP c.2483+6 T>G using the SD-Score (E) or MaxEntScan (F) programs; G. Segments of multiple sequence alignments of *CYLD* protein from different species were shown using the PolyPhen-2 program. The position of the changed amino acid (p.W736) in *CYLD* protein is marked in a bold solid line box.

Pos – position; Wt.Seq – wild-type sequence; Mt.Seq – mutant sequence; SD-Score – a common logarithm of the frequency of a specific 5'splice site in human genes; Ri – information contents; CV – position weight matrix; MaxENT – Maximum Entropy Model; MDD – Maximum Dependence Decomposition Model; MM – Markov Model; WMM – Weight Matrix Model.

while the 10 other SNPs in *CYLD* gene were not significantly associated with PV phenotype. The evidence revealed the association of the W736G nsSNP in susceptibility to the progression of PV.

For the analysis of the possible impact of the 5 intronic SNPs in *CYLD* gene on splicing, only the SNP

c. 2483+6 T>G was predicted as an aberrant splicing according to the SD-Score prediction program (Fig. 2E).³¹ Besides, the MaxEntScan³² splicing prediction through the score analysis of MaxENT (Maximum Entropy Model), MDD (Maximum Dependence Decomposition Model), MM (First-order Markov Model), and WMM

Table 1. General information on single nucleotide polymorphisms (SNPs) of *JAK2*, *CYLD*, *A20* and *Cezanne* genes in polycythemia vera (PV) patients and controls

Gene/SNP	Position	Type of variant	Allele	MAF in PV group	HWE in PV group (p)	MAF in control group	HWE in control group (p)	HWE in all population (p)
<i>JAK2</i> /rs77375493	9:5073770	missense	G>T	0.442	0.656	0	NaN	0.051
<i>CYLD</i> /c.2351-118	16:50791440	intron	Del A	0	0.993	0	0.913	0.938
<i>CYLD</i> /c.2351-31	16:50791527	intron	T>G	0.006	0.998	0	NaN	0.999
<i>CYLD</i> /c.2355 p.A705P	16:50791562	missense	G>C	0.020	0.985	0	NaN	0.991
<i>CYLD</i> /c.2411 p.E723E	16:50791618	synonymous	G>A	0.033	0.958	0.055	0.913	0.883
<i>CYLD</i> /c.2435 p.Q731H	16:50791642	missense	G>C	0.111	0.553	0.137	0.504	0.285
<i>CYLD</i> /c.2445 p.E735K	16:50791652	missense	G>A	0.130	0.424	0.173	0.302	0.138
<i>CYLD</i> /c.2448 p.W736G	16:50791655	missense	T>G	0.091	0.681	0.010	0.998	0.787
<i>CYLD</i> /c.2481 p.E747K	16:50791688	missense	G>A	0.169	0.204	0.219	0.118	0.027
<i>CYLD</i> /c.2483+6	16:50791696	splice-donor-site	T>G	0.026	0.973	0	NaN	0.985
<i>CYLD</i> /c.2483 +39	16:50791729	intron	T>G	0.039	0.939	0.010	0.998	0.952
<i>CYLD</i> /c.2483+53	16:50791743	intron	G>A	0.182	0.149	0.219	0.118	0.019
<i>A20</i> /rs776591390	6:137878495	missense	G>T	0.006	0.998	0	NaN	0.999
<i>A20</i> /rs141376366	6:137878670	synonymous	G>A	0	NaN	0.010	0.998	0.999
<i>A20</i> /rs745670694	6:137878786	synonymous	G>A	0	NaN	0.108	0.991	0.996
<i>Cezanne</i> /c.1584-287	1:149947622	intron	C>G	0.039	0.998	0	NaN	0.965
<i>Cezanne</i> /rs1168285629	1:149947587	intron	A>G	0.046	0.916	0.019	0.991	0.921
<i>Cezanne</i> /rs1394369937	1:149947537	intron	A>G	0.026	0.973	0	NaN	0.985
<i>Cezanne</i> /c.1584-167	1:149947502	intron	G>T	0.013	0.993	0	NaN	0.996
<i>Cezanne</i> /c.1584-122	1:149947457	intron	G>T	0.026	0.973	0.010	0.998	0.976
<i>Cezanne</i> /rs1158787149	1:149947449	intron	C>G	0.026	0.987	0	NaN	0.985
<i>Cezanne</i> /rs1553772411	1:149947450	intron	C>G	0.019	0.993	0	NaN	0.991

Position refers to the GRCh38.p10 assembly. MAF – minor allele frequency; HWE – Hardy–Weinberg equilibrium (checked using χ^2 test).

(Weight Matrix Model) indicated that the mutant scores of the SNP c.2483+6 T>G were lower than of the wild-type scores (Fig. 2F), suggesting that the SNP c.2483+6 T>G may be a splice-donor-site mutation.

Further analysis of an alignment of CYLD protein using the PolyPhen-2 software showed that the p.W736 residue is a highly conserved site among different species, including humans (*Homo sapiens*), rat (*Rattus norvegicus*), gray short-tailed opossum (*Monodelphis domestica*), Tasmanian devil (*Sarcophilus harrisii*), duckbill platypus (*Ornithorhynchus anatinus*), little brown bat (*Myotis lucifugus*), chicken (*Gallus gallus*), wild turkey (*Meleagris gallopavo*), western clawed frog (*Xenopus tropicalis*), Nile tilapia (*Oreochromis niloticus*), zebrafish (*Danio rerio*), three-spined stickleback (*Gasterosteus aculeatus*), African elephant (*Loxodonta africana*), and spotted green pufferfish (*Tetraodon nigroviridis*) (Fig. 2G).

Next, the sequencing of *A20* gene identified 3 nucleotide changes, including rs776591390 G>T, rs141376366 G>A and rs745670694 G>A, in exon 7 (Fig. 3). The genotype distributions of the 3 SNPs in this gene were in accordance with HWE ($p > 0.05$) (Table 1). The MAF for the SNP rs776591390 was slightly higher, whereas the MAFs for the 2 remaining SNPs were lower in PV patients than

in the control group. Among the 3 SNPs, the missense SNP rs776591390 of *A20* gene was identified in 1 out of 77 PV patients (1.81%) and the 2 remaining SNPs rs141376366 and rs745670694 were found only in control individuals with the carrier frequencies of 1.81% and 3.63%, respectively (Table 2).

Finally, the sequencing of *Cezanne* gene identified 7 nucleotide changes in intron 10, 3 out of the 7 intronic SNPs (c.1584-287 C>G, c.1584-167 G>T and c.1584-122 G>T) were unidentified SNPs and the 4 remaining intronic SNPs (rs1168285629 A>G, rs1394369937 A>G, rs1158787149 C>G, and rs1553772411 C>G) are reported in NCBI SNP database (Fig. 4). The genotype distributions of the 7 SNPs in *Cezanne* gene were in accordance with HWE ($p > 0.05$) (Table 1). The MAFs of the 7 intronic SNPs were slightly higher in the PV group than in healthy individuals. Among these SNPs, 5 out of the 7 intronic SNPs (c.1584-287 C>G, rs1394369937 A>G, c.1584-167 G>T, rs1158787149 C>G and rs1553772411 C>G) appeared in PV patients, but not in the control group, with the carrier frequencies of 7.79%, 5.19%, 2.6%, 5.19%, and 3.89%, respectively (Table 2). Importantly, 7 out of 77 (9.09%) PV patients carried at least 2 SNPs in *Cezanne* gene.

Table 2. Comparison of genotype frequencies of *JAK2*, *CYLD*, *A20*, and *Cezanne* genes between polycythemia vera (PV) patients and controls

SNP	Gene	Test model	Controls (n = 55)	PV patients (n = 77)	p-value
<i>rs77375493</i>	<i>JAK2</i>	GG	55 (100%)	26 (33.76%)	<0.001⁽²⁾
		GT/TT	0 (0%)	51 (66.24%)	
<i>c.2351-118</i>	<i>CYLD</i>	AA	49 (89.09%)	75 (97.4%)	0.052 ⁽¹⁾
		DelA	6 (10.91%)	2 (2.6%)	
<i>c.2351-31</i>	<i>CYLD</i>	TT	55 (100%)	76 (98.7%)	1 ⁽¹⁾
		TG	0	1 (1.3%)	
<i>c.2355 p.A705P</i>	<i>CYLD</i>	GG	55 (100%)	74 (96.1%)	0.121 ⁽¹⁾
		GC	0 (0%)	3 (3.9%)	
<i>c.2411 p.E723E</i>	<i>CYLD</i>	GG	49 (89.09%)	72 (93.5%)	0.335 ⁽¹⁾
		GA	6 (10.91%)	5 (6.5%)	
<i>c.2435 p.Q731H</i>	<i>CYLD</i>	GG	40 (72.73%)	60 (77.9%)	0.511 ⁽¹⁾
		GC	15 (27.27%)	17 (22.1%)	
<i>c.2445 p.E735K</i>	<i>CYLD</i>	GG	36 (65.46%)	57 (44%)	0.055 ⁽¹⁾
		GA	19 (34.54%)	20 (56%)	
<i>c.2448 p.W736G</i>	<i>CYLD</i>	TT	54 (98.19%)	63 (81.8%)	<0.001⁽¹⁾
		TG	1 (1.81%)	14 (18.2%)	
<i>c.2481 p.E747K</i>	<i>CYLD</i>	GG	31 (56.36%)	51 (66.2%)	0.147 ⁽²⁾
		GA	24 (43.64%)	26 (33.8%)	
<i>c.2483+6</i>	<i>CYLD</i>	TT	55 (100%)	73 (94.8%)	0.059 ⁽¹⁾
		TG	0 (0%)	4 (5.2%)	
<i>c.2483+39</i>	<i>CYLD</i>	TT	54 (98.19%)	71 (92.2%)	0.101 ⁽¹⁾
		TG	1 (1.81%)	6 (7.8%)	
<i>c.2483+53</i>	<i>CYLD</i>	GG	31 (56.37%)	49 (63.6%)	0.248 ⁽²⁾
		GA	24 (43.63%)	28 (36.4%)	
<i>rs776591390</i>	<i>A20</i>	GG	55 (100%)	76 (98.71%)	1 ⁽¹⁾
		TG	0	1 (1.29%)	
<i>rs141376366</i>	<i>A20</i>	GG	54 (98.19%)	77 (100%)	0.497 ⁽¹⁾
		GA	1 (1.81%)	0	
<i>rs745670694</i>	<i>A20</i>	GG	53 (96.37%)	77 (100%)	0.121 ⁽¹⁾
		AG	2 (3.63%)	0 (0%)	
<i>c.1584-287</i>	<i>Cezanne</i>	CC	55 (100%)	71 (92.21%)	0.007⁽¹⁾
		CG	0 (0%)	6 (7.79%)	
<i>rs1168285629</i>	<i>Cezanne</i>	AA	53 (96.36%)	70 (90.91%)	0.251 ⁽¹⁾
		AG	2 (3.64%)	7 (9.09%)	
<i>rs1394369937</i>	<i>Cezanne</i>	AA	55 (100%)	73 (94.81%)	0.059 ⁽¹⁾
		AG	0 (0%)	4 (5.19%)	
<i>c.1584-167</i>	<i>Cezanne</i>	GG	55 (100%)	75 (97.4%)	0.246 ⁽¹⁾
		GT	0 (0%)	2 (2.60%)	
<i>c.1584-122</i>	<i>Cezanne</i>	GG	54 (98.18%)	73 (94.81%)	0.445 ⁽¹⁾
		GT	1 (1.82%)	4 (5.19%)	
<i>rs1158787149</i>	<i>Cezanne</i>	CC	55 (100%)	73 (94.81%)	0.059 ⁽¹⁾
		CG	0 (0%)	4 (5.19%)	
<i>rs1553772411</i>	<i>Cezanne</i>	CC	55 (100%)	74 (96.11%)	0.121 ⁽¹⁾
		CG	0 (0%)	3 (3.89%)	

The p-values were calculated using either Fisher's exact test ⁽¹⁾ or χ^2 test ⁽²⁾; p < 0.05 (in bold) indicates statistical significance from genotype frequencies of healthy donors.

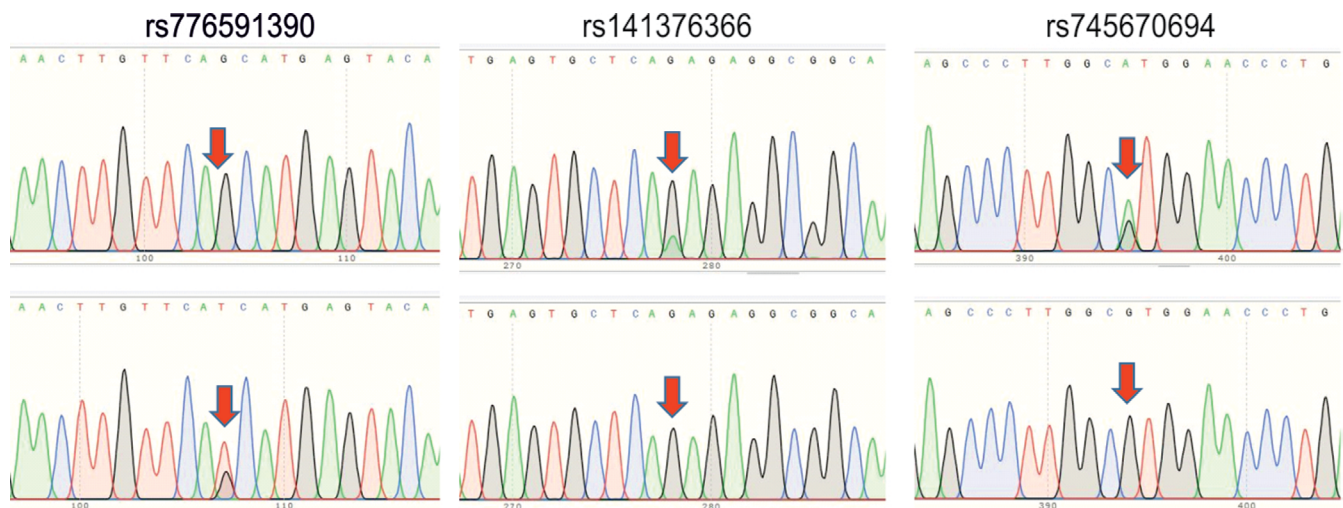


Fig. 3. Polymorphisms of *A20* gene in polycythemia vera (PV) patients and controls. Partial sequence chromatograms of *A20* gene from healthy individuals (upper panels) and PV patients (lower panels), in which the rs776591390, rs141376366 and rs745670694 polymorphisms are shown. Arrows indicate the location of the base changes

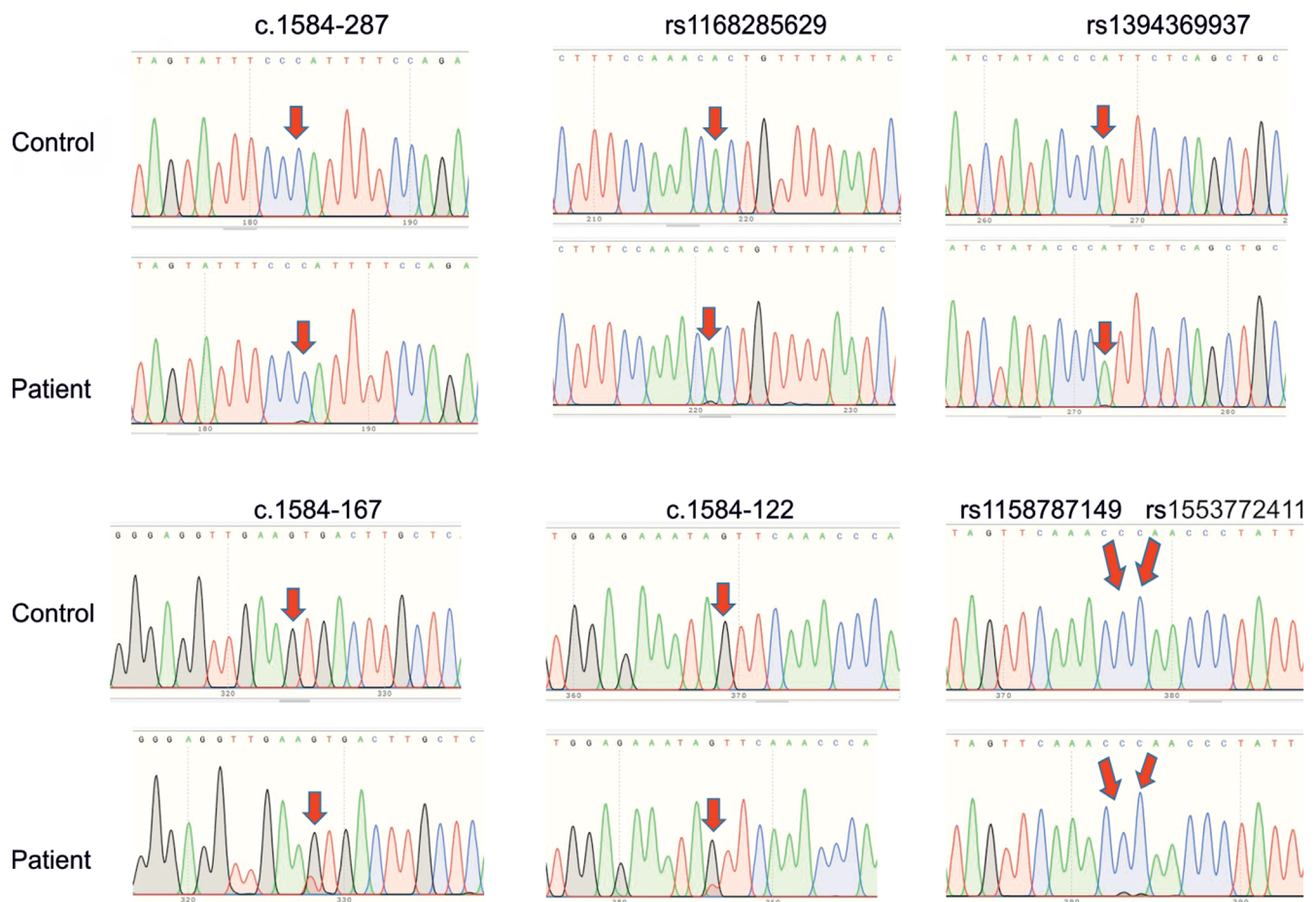


Fig. 4. Polymorphisms of *Cezanne* gene in polycythemia vera (PV) patients and controls. Partial sequence chromatograms of *Cezanne* gene from healthy individuals (upper panels) and PV patients (lower panels), in which the c.1584-287 C>G, rs1168285629 A>G, rs1394369937 A>G, c.1584-167 G>T, c.1584-122 G>T, rs1158787149 C>G, and rs1553772411 C>G polymorphisms are shown. Arrows indicate the location of the base changes

Association between the different SNPs in *JAK2* and the DUB genes in PV patients

For determination of the correlation among the SNPs in *JAK2* and the DUB genes, we observed that 10 out

of 14 (71.4%) PV cases carrying the W736G nsSNP and 3 out of 3 (100%) carriers of the intronic SNP c. 2483+6 T>G in *CYLD* gene were positive for the *JAK2*^{V617F} mutation (data not shown), whereas, the *JAK2*^{V617F}-positive rate of PV carriers of the other SNPs in the DUB genes were similar

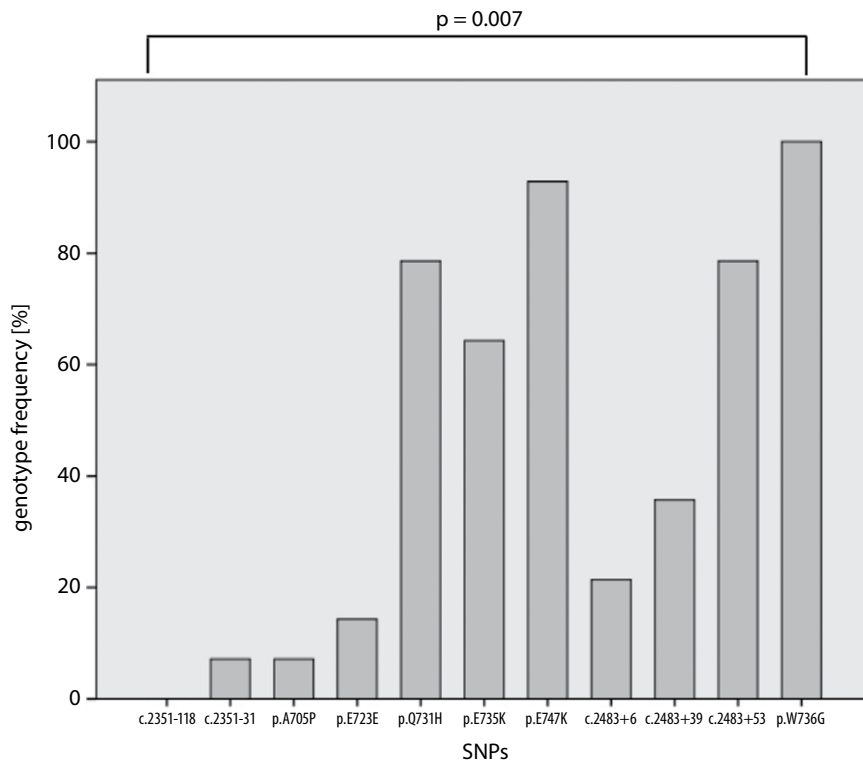


Fig. 5. The relevance of polycythemia vera (PV) carriers of the W736G nsSNP and the other 9 SNPs in *CYLD* gene. The p-value was calculated using Kruskal–Wallis test (K related samples); $p = 0.007$ indicates a significant relevance among the single nucleotide polymorphisms (SNPs) in *CYLD* gene

to healthy individuals (data not shown). The evidence indicated that there was a significant positive correlation between PV carriers of the W736G nsSNP or/and the intronic SNP c.2483+6 T>G and PV patients with JAK2^{V617F} mutation.

Interestingly, out of the 14 patients carrying the W736G nsSNP in *CYLD* gene, 13 (92.8%) cases were found to carry the SNP p.E747K; 11 (78.6%) cases had both the SNP p.Q731H G>C and the SNP c.2483+53 G>A; 9 (64.3%) cases were found to carry the SNP p.E735K; and 3 (21.4%) carriers of the SNP c.2483+6 T>G and 5 (35.7%) cases infected with the SNP c.2483+39 T>G were observed (Fig. 5). According to the Kruskal–Wallis test results, significant relevance was observed among the SNPs in *CYLD* gene ($\chi^2=7.364$, $p = 0.007$), suggesting that PV carriers of the W736G nsSNP had multiple SNPs in *CYLD* gene. Additionally, we observed that PV carriers of the W736G nsSNP and the intronic SNP c.2483+6 T>G in *CYLD* gene did not have SNP in *A20* or *Cezanne* gene (Fig. 5).

Discussion

In this study, inactivated expression of *A20*, *Cezanne* and *CYLD* in PV patients was revealed for the first time. Among the DUB genes, *A20* and *CYLD* but not *Cezanne* are known as inhibitors of immune reaction through JAK/STAT signaling, whose activation results in the development and pathogenesis of leukemia and lymphoma, including PV.^{4,5} A recent study reported that the aberrant expression and mutations in *CYLD* gene are associated with the susceptibility to leukemia and lymphoma.^{12,15} Among the 11 SNPs examined in *CYLD* genes, W736G nsSNP was found to be

most likely to exert deleterious effect – it was observed using the PolyPhen-2 prediction tool and the intronic SNP c.2483+6 T>G was identified as an aberrant splicing by the SD-Score or MaxEntScan predictor program. Importantly, the 2 aberrant SNPs were not found in all samples from 90 patients with chronic myeloid leukemia (CML), 32 patients with acute myeloid leukemia (AML), 16 patients with acute lymphoblastic leukemia (ALL), and 21 patients with chronic lymphocytic leukemia (CLL) (unpublished data), suggesting that the two SNPs could be associated with significant risk of PV, but not leukemia.

Investigations on genetic alteration of *A20* gene indicated that carriers of SNPs in the *A20* gene at exons 5, 6 and 7 are at high risk for autoinflammatory disease and lymphocytic leukemia.^{10,11,35,36} In this study, the SNP rs776591390 in *A20* gene was detected in PV patients with the frequency of 1.29%, pointing out that *A20* polymorphisms associated with disease susceptibility are different.

Unlike the impact of *A20* and *CYLD*, the involvement of SNPs in *Cezanne* gene with the possible risk of leukemia is not fully documented, although *Cezanne* expression is linked to poor prognosis in hepatocellular carcinoma.²⁰ In this study, we also revealed for the first time that changes of 7 nucleotides at intron 10 in *Cezanne* gene were found in PV patients and in 7 out of 77 (9.09%) PV patients who carried at least the 2 SNPs in this gene. Similar to the 2 aberrant SNPs in *CYLD* gene, the 7 intronic SNPs in *Cezanne* gene were not carried by AML and CML patients (unpublished data). In addition, the MAFs of the 7 intronic SNPs had slightly higher frequencies in PV groups than in control groups, indicating that carriers of SNPs in *Cezanne* gene could tend to be at risk of the progression of PV.

In addition to the determination of DNA sequences of the DUB genes, the presence of the *JAK2V617F* mutation in PV patients was also conducted to determine the correlation between SNPs in the *JAK2* and the DUB genes. The *JAK2V617F* mutation was detected in 66.67% of PV patients in this study, whereas other study indicated the presence of this mutation is about 90% of PV cases.³ The frequency of *JAK2V617F* allele burden is known to time-dependently increase in PV cases.³⁷ A recent study indicated that the absence of the *JAK2V617F* mutation in PV patients does not affect treatment effectiveness with JAK/STAT pathway inhibitors,³⁸ suggesting that the constitutive activation of the JAK-STAT pathway could be caused by not only *JAK2V617F* mutation. Besides the known mutations involved in the pathogenesis of PV, including *JAK2*, *MPL* and *CALR*, we additionally revealed that PV patients carrying the W736G nsSNP had multiple SNPs in the *CYLD*, but not in *A20* or *Cezanne* gene, suggesting that the effect of the W736G nsSNP in *CYLD* gene might be one of potential treatment targets for PV. The *CYLD* is known to suppress inflammatory reaction through the activation of several pathways, including JAK/STAT⁷; therefore, further studies would investigate the effects of the W736G nsSNP in regulating function of PV cells and underlying mechanisms.

In the analysis of involvement in SNPs and immunophenotype in PV patients, the *JAK2V617F* mutation is reported not to affect the function of T cells³; therefore, the recruitment of CD25⁺CD4T, Th1 and Treg cells into the circulatory system in PV cases would be related to the activation of the 2 aberrant SNPs in *CYLD* gene. Importantly, the enhanced activation of Th1 cells in PV cells was also revealed for the first time in our study. As part of the immune response, Treg cells play an important role in suppressing tumor-specific immunity.³⁰ The aberrant expression of CD25 is associated with poor prognosis in AML⁴⁰ and CML.⁴¹ A previous study indicated that factors related to thrombosis in PV include increased hematocrit, thrombocytosis, platelet activation, and leukocyte activation,⁴² suggesting the regulatory effects of the 2 aberrant SNPs in *CYLD* gene on the development of thrombosis in PV. In addition, we did not find any significant association of the SNPs in *A20* and *CYLD* and *Cezanne* genes with increased levels of IL-6 and TNF- α in PV patients.

Limitations

There are some limitations to the current study. First, the sample size was not sufficient to verify a potential association between the SNPs in the DUB genes and risk of PV disease in the Vietnamese population. Second, further functional research is necessary for investigating the impacts of the W736G nsSNP and/or intronic SNP c.2483+6 T>G in *CYLD* gene on PV cell activation for the development of PV treatment. Finally, we only

examined number and activation of myeloid (CD11b⁺) and CD4 T cells present in PV cells, while other cell types, such as macrophages, inflammatory monocytes and B cells, might be also related to the activation of the 2 aberrant SNPs in *CYLD* gene.

Conclusions

The deleterious effect of the W736G nsSNP in *CYLD* gene could contribute to the pathogenesis of PV and be a good candidate for further study on its role in regulating functional activation of PV cells.

ORCID iDs

Do Thi Trang  <https://orcid.org/0000-0002-3168-1000>
 Nguyen Hoang Giang  <https://orcid.org/0000-0002-8298-3017>
 Bui Kieu Trang  <https://orcid.org/0000-0001-8285-1412>
 Nguyen Thy Ngoc  <https://orcid.org/0000-0002-3181-9209>
 Nguyen Thi Xuan  <https://orcid.org/0000-0003-3494-5136>

References

- Arber DA, Orazi A, Hasserjian R, et al. The 2016 revision to the World Health Organization classification of myeloid neoplasms and acute leukemia. *Blood*. 2016;127(20):2391–1405. doi:10.1182/blood-2016-03-643544
- Barbui T, Thiele J, Gisslinger H, et al. The 2016 WHO classification and diagnostic criteria for myeloproliferative neoplasms: Document summary and in-depth discussion. *Blood Cancer J*. 2018;8(2):15. doi:10.1038/s41408-018-0054-y
- James C, Ugo V, Le Couedic JP, et al. A unique clonal JAK2 mutation leading to constitutive signalling causes polycythaemia vera. *Nature*. 2005;434(7037):1144–1148. doi:10.1038/nature03546
- Levine RL, Pardanani A, Tefferi A, Gilliland DG. Role of JAK2 in the pathogenesis and therapy of myeloproliferative disorders. *Nat Rev Cancer*. 2007;7(9):673–683. doi:10.1038/nrc2210
- Tefferi A. Myeloproliferative neoplasms: A decade of discoveries and treatment advances. *Am J Hematol*. 2016;91(1):50–58. doi:10.1002/ajh.24221
- Duy PN, Thuy NT, Trang BK, et al. Regulation of NF-kappaB- and STAT1-mediated plasmacytoid dendritic cell functions by A20. *PLoS One*. 2019;14(9):e0222697. doi:10.1371/journal.pone.0222697
- Nishanth G, Deckert M, Wex K, et al. CYLD enhances severe listeriosis by impairing IL-6/STAT3-dependent fibrin production. *PLoS Pathog*. 2013;9(6):e1003455. doi:10.1371/journal.ppat.1003455
- Compagno M, Lim WK, Grunn A, et al. Mutations of multiple genes cause deregulation of NF-kappaB in diffuse large B-cell lymphoma. *Nature*. 2009;459(7247):717–721. doi:10.1038/nature07968
- Kato M, Sanada M, Kato I, et al. Frequent inactivation of A20 in B-cell lymphomas. *Nature*. 2009;459(7247):712–716. doi:10.1038/nature07969
- Zhu L, Zhang F, Shen Q, et al. Characteristics of A20 gene polymorphisms in T-cell acute lymphocytic leukemia. *Hematology*. 2014;19(8):448–454. doi:10.1179/1607845414Y.0000000160
- Philipp C, Edelmann J, Buhler A, et al. Mutation analysis of the TNFAIP3 (A20) tumor suppressor gene in CLL. *Int J Cancer*. 2011;128(7):1747–1750. doi:10.1002/ijc.25497
- Arora M, Kaul D, Varma N. Functional nature of a novel mutant CYLD observed in pediatric lymphoblastic B-cell leukemia. *Pediatr Blood Cancer*. 2015;62(6):1066–1069. doi:10.1002/pbc.25387
- Johari T, Maiti TK. Catalytic domain mutation in CYLD inactivates its enzyme function by structural perturbation and induces cell migration and proliferation. *Biochim Biophys Acta Gen Subj*. 2018;1862(9):2081–2089. doi:10.1016/j.bbagen.2018.05.016
- Massoumi R. CYLD: A deubiquitination enzyme with multiple roles in cancer. *Future Oncol*. 2011;7(2):285–297. doi:10.2217/fon.10.187
- Wu W, Zhu H, Fu Y, et al. Clinical significance of down-regulated cylindromatosis gene in chronic lymphocytic leukemia. *Leuk Lymphoma*. 2014;55(3):588–594. doi:10.3109/10428194.2013.809077

16. Liu P, Xu B, Shen W, et al. Dysregulation of TNF α -induced necroptotic signaling in chronic lymphocytic leukemia: Suppression of CYLD gene by LEF1. *Leukemia*. 2012;26(6):1293–1300. doi:10.1038/leu.2011.357
17. Xu X, Kalac M, Markson M, et al. Reversal of CYLD phosphorylation as a novel therapeutic approach for adult T-cell leukemia/lymphoma (ATLL). *Cell Death Dis*. 2020;11(2):94. doi:10.1038/s41419-020-2294-6
18. Ye H, Liu X, Lv M, et al. MicroRNA and transcription factor co-regulatory network analysis reveals miR-19 inhibits CYLD in T-cell acute lymphoblastic leukemia. *Nucleic Acids Res*. 2012;40(12):5201–5214. doi:10.1093/nar/gks175
19. Enesa K, Zakkar M, Chaudhury H, et al. NF-kappaB suppression by the deubiquitinating enzyme Cezanne: A novel negative feedback loop in pro-inflammatory signaling. *J Biol Chem*. 2008;283(11):7036–7045. doi:10.1074/jbc.M708690200
20. Wang JH, Wei W, Guo ZX, Shi M, Guo RP. Decreased Cezanne expression is associated with the progression and poor prognosis in hepatocellular carcinoma. *J Transl Med*. 2015;13:41. doi:10.1186/s12967-015-0396-1
21. Lin DD, Shen Y, Qiao S, et al. Upregulation of OTUD7B (Cezanne) promotes tumor progression via AKT/VEGF pathway in lung squamous carcinoma and adenocarcinoma. *Front Oncol*. 2019;9:862. doi:10.3389/fonc.2019.00862
22. Hasselbalch HC. Perspectives on chronic inflammation in essential thrombocythemia, polycythemia vera, and myelofibrosis: Is chronic inflammation a trigger and driver of clonal evolution and development of accelerated atherosclerosis and second cancer? *Blood*. 2012;119(14):3219–3225. doi:10.1182/blood-2011-11-394775
23. Lee EG, Boone DL, Chai S, et al. Failure to regulate TNF-induced NF-kappaB and cell death responses in A20-deficient mice. *Science*. 2000;289(5488):2350–2354. doi:10.1126/science.289.5488.2350
24. Jin W, Reiley WR, Lee AJ, et al. Deubiquitinating enzyme CYLD regulates the peripheral development and naive phenotype maintenance of B cells. *J Biol Chem*. 2007;282(21):15884–15893. doi:10.1074/jbc.M609952200
25. Reiley WW, Zhang M, Jin W, et al. Regulation of T cell development by the deubiquitinating enzyme CYLD. *Nat Immunol*. 2006;7(4):411–417. doi:10.1038/ni1315
26. Zhao WB, Li Y, Liu X, Zhang LY, Wang X. Involvement of CD4⁺CD25⁺ regulatory T cells in the pathogenesis of polycythaemia vera. *Chin Med J (Engl)*. 2008;121(18):1781–1786. PMID:19080357.
27. Baxter EJ, Scott LM, Campbell PJ, et al. Acquired mutation of the tyrosine kinase JAK2 in human myeloproliferative disorders. *Lancet*. 2005;365(9464):1054–1061. doi:10.1016/S0140-6736(05)71142-9
28. Livak KJ, Schmittgen TD. Analysis of relative gene expression data using real-time quantitative PCR and the 2^{(-delta delta C(T))} method. *Methods*. 2001;25(4):402–408. doi:10.1006/meth.2001.1262
29. Song LH, Toan NL, Xuan NT, et al. A promoter polymorphism in the *interferon alpha-2* gene is associated with the clinical presentation of hepatitis B. *Mutat Res*. 2006;601(1–2):137–143. doi:10.1016/j.mrfmmm.2006.06.011
30. Ohno K, Takeda JI, Masuda A. Rules and tools to predict the splicing effects of exonic and intronic mutations. *Wiley Interdiscip Rev RNA*. 2018;9(1). doi:10.1002/wrna.1451
31. Jian X, Boerwinkle E, Liu X. In silico tools for splicing defect prediction: A survey from the viewpoint of end users. *Genet Med*. 2014;16(7):497–503. doi:10.1038/gim.2013.176
32. Xuan NT, Wang X, Nishanth G, et al. A20 expression in dendritic cells protects mice from LPS-induced mortality. *Eur J Immunol*. 2015;45(3):818–828. doi:10.1002/eji.201444795
33. Pourcelot E, Trocme C, Mondet J, et al. Cytokine profiles in polycythemia vera and essential thrombocythemia patients: Clinical implications. *Exp Hematol*. 2014;42(5):360–368. doi:10.1016/j.exphem.2014.01.006
34. Canh NX, Giang NV, Nghia VX, et al. Regulation of cell activation by A20 through STAT signaling in acute lymphoblastic leukemia. *J Recept Signal Transduct Res*. 2021;41(4):331–338. doi:10.1080/10799893.2020.1808678
35. Birgen D, Ertem U, Duru F, et al. Serum Ca 125 levels in children with acute leukemia and lymphoma. *Leuk Lymphoma*. 2005;46(8):1177–1181. doi:10.1080/10428190500096690
36. Johansson P, Bergmann A, Rahmann S, et al. Recurrent alterations of TNFAIP3 (A20) in T-cell large granular lymphocytic leukemia. *Int J Cancer*. 2016;138(1):121–124. doi:10.1002/ijc.29697
37. Zhou Q, Wang H, Schwartz DM, et al. Loss-of-function mutations in TNFAIP3 leading to A20 haploinsufficiency cause an early-onset autoinflammatory disease. *Nat Genet*. 2016;48(1):67–73. doi:10.1038/ng.3459
38. Tefferi A, Strand JJ, Lasho TL, et al. Bone marrow JAK2V617F allele burden and clinical correlates in polycythemia vera. *Leukemia*. 2007;21(9):2074–2075. doi:10.1038/sj.leu.2404724
39. Tefferi A, Barbui T. Polycythemia vera and essential thrombocythemia: 2019 update on diagnosis, risk-stratification and management. *Am J Hematol*. 2019;94(1):133–143. doi:10.1002/ajh.25303
40. Schabowsky RH, Madireddi S, Sharma R, Yolcu ES, Shirwan H. Targeting CD4⁺CD25⁺FoxP3⁺ regulatory T-cells for the augmentation of cancer immunotherapy. *Curr Opin Investig Drugs*. 2007;8(12):1002–1008. PMID:18058571.
41. Cerny J, Yu H, Ramanathan M, et al. Expression of CD25 independently predicts early treatment failure of acute myeloid leukaemia (AML). *Br J Haematol*. 2013;160(2):262–266. doi:10.1111/bjh.12109
42. Blatt K, Menzl I, Eisenwort G, et al. Phenotyping and target expression profiling of CD34(+)/CD38(–) and CD34(+)/CD38(+) stem and progenitor cells in acute lymphoblastic leukemia. *Neoplasia*. 2018;20(6):632–642. doi:10.1016/j.neo.2018.04.004
43. Kwaan HC, Wang J. Hyperviscosity in polycythemia vera and other red cell abnormalities. *Semin Thromb Hemost*. 2003;29(5):451–458. doi:10.1055/s-2003-44552